Frontiers Med. Biol. Engng, Vol. 11, No. 1, pp. 13–29 (2001)

Original paper

Automatic analysis and classification of surface electromyography

FATMA E. Z. ABOU-CHADI*, AYMAN NASHAR[1] and MOHAMED SAAD[2]

[1] *Department of Electronics and Communications Engineering, Mansoura University, P.O. 35516, Box 20, Mansoura, Egypt*
[2] *Department of Neurology, Faculty of Medicine, Mansoura University, P.O. 35516, Box 20, Mansoura, Egypt*

Received 22 November 1999; revised 12 June 2000; accepted 22 August 2000

Abstract—In this paper, parametric modeling of surface electromyography (EMG) algorithms that facilitates automatic SEMG feature extraction and artificial neural networks (ANN) are combined for providing an integrated system for the automatic analysis and diagnosis of myopathic disorders. Three paradigms of ANN were investigated: the multilayer backpropagation algorithm, the self-organizing feature map algorithm and a probabilistic neural network model. The performance of the three classifiers was compared with that of the old Fisher linear discriminant (FLD) classifiers. The results have shown that the three ANN models give higher performance. The percentage of correct classification reaches 90%. Poorer diagnostic performance was obtained from the FLD classifier. The system presented here indicates that surface EMG, when properly processed, can be used to provide the physician with a diagnostic assist device.

Key words: Biological signal processing; surface electromyography; automatic classification; autoregressive modeling; neural networks.

1. INTRODUCTION

Electromyography (EMG) is the study of the electrical activity of muscle and forms a valuable aid in the diagnosis of neuromuscular disorders. EMG findings are used to detect and describe different disease processes affecting the motor unit, the smallest functional unit of the muscle. With voluntary muscle contraction, the action potential reflecting the electrical activity of a single anatomical motor unit can be recorded. It is the compound motor unit action potential (MUAP) of those muscle fibers within the recording range of the needle or surface electrodes [1].

*To whom correspondence should be addressed. E-mail: f-abochadi@ieee.org

The MUAP waveform depends on the motor unit architecture, i.e. on the number of fibers, their sizes and density, so the analysis of MUAP shape may provide important information about the motor unit structure and its changes. The disease processes which affect the structure and activity of the motor unit are reflected in the changes of MUAP features, particularly those of the durations and amplitudes. These changes may also manifest themselves as polyphasic potentials [2] characterized by an increased number of phases and/or turns, i.e. in signals of a more complicated shape than the normal MUAP. The changes of the MUAP shape are an important indicator of motor unit disintegration and compensatory processes [3].

Recently, several authors successfully investigated muscle properties by analyzing the time course of amplitude parameters, muscle fiber conduction velocity and spectral parameters of the EMG signal during voluntary and electrically elicited isometric contractions [4, 5].

It is also well known and documented that the power spectral density function of the EMG signal undergoes frequency compression during either voluntary or electrically elicited sustained contractions [6], long before the muscle becomes unable to produce the desired force. Such changes are referred to as myoelectric manifestations of localized muscle fatigue.

The spectral content of the EMG signal depends on (i) the number of active motor units whose electrical activity is sensed by the detection probe, (ii) their firing rates, (iii) the position of the active muscle fibers relative to the detection probe and (iv) the velocity of propagation of depolarization along muscle fibers [7]. During a sustained muscle contraction, the spectral compression is mainly due to a progressive reduction of muscle fiber conduction velocity and to the variation of the spatial distribution of depolarization along the muscle fibers [8]. Therefore, if spectral parameters are studied, it is important to separate their random variations due to estimation errors from those due to physiological events.

Previous approaches for analyzing the time-varying aspects of the EMG signals have used a linear prediction model. Among them, the autoregressive (AR) model has been used to deal with time-varying EMG signals because it emphasizes spectral peaks for time records having a small number of samples [9]. This approach was introduced by Graupe and Cline [10] who attempted to use the surface EMG signal for controlling prostheses. Subsequently, Sherif *et al.* [11] studied the behavior of AR integrated moving average (ARIMA) coefficients of the EMG signal from the deltoid muscle during dynamic contractions. Capponi *et al.* [12] represented EMG signals, detected from the biceps and triceps muscles, with the time courses of AR coefficients during rapid isometric contractions. Recently, Kiryu *et al.* [13] investigated the physiological interpretation of AR modeling. They analyzed the time-varying behavior of AR parameters of well-conditioned EMG signals detected during an isometric force-varying ramp contraction. The AR coefficients of the EMG signal could be used as quantitative measures to monitor local muscle fatigue [14, 15].

To further the development of quantitative EMG techniques, the need has emerged for adding automated decision-making support to these techniques so that all data is processed in an integrated environment. Towards this goal, Coatrieux *et al.* [16] applied cluster analysis for the automatic diagnosis of pathology based on MUAP records. Hassoun *et al.* [17] proposed automated EMG signal decomposition using neural networks. Pattichis *et al.* [18] utilized artificial neural networks (ANNs) for the automatic classification of EMG features recorded using needle electrodes for normal individuals and patients suffering from neuromuscular diseases. They used seven features derived from the shape of the MUAP waveforms.

The main goal of the present work is threefold: to assure the usage of surface EMG (SEMG) in clinical diagnosis, to characterize the SEMG signal through the determination of the AR model parameters to be used for comparisons between groups of patients or between an individual record and any population norms that might become available, and to provide an efficient classification for the different pathological cases.

The classification approaches taken here are: the old Fisher linear discriminant (FLD) algorithm and three models of neural networks: the multilayer back-propagation model, the self-organizing feature map (SOM) model and a probabilistic neural network (PNN) model. A comparison of the performance of the four classifiers is performed for normal individuals and patients suffering with myopathic lesions.

2. DATA ACQUISITION

Twenty-eight subjects were used in this work: 14 normals and 14 suffering from myopathy. SEMG signal was recorded from the deltoid muscle at 50% maximum voluntary contraction (MVC) for 5 s using bipolar surface electrodes. The recording points within the muscle are standardized. The Biopac data acquisition system consists of an internal microprocessor MP100 data acquisition card with 16 analog input channels connected to an Apple PC. The software used in data acquisition is Acqknowledge version 2 software. Figure 1 illustrates examples of the SEMG signals.

2.1. The sampling frequency

It is known that information exists in the EMG frequency spectrum up to frequencies of 1 kHz, implying that in order to satisfy the Nyquist criterion, a sampling frequency of at least 2 kHz would have to be used. However, for surface myoelectric signals, most of the power in the signal is at low frequencies (below 300 Hz).

Further, consideration of average autocorrelation functions of the EMG recorded in a myopathic subject and a normal subject taken from a pair of surface electrodes placed over motor unit of the deltoid muscle indicates that the difference between these functions is more pronounced at low frequencies. Figure 2 illustrates the

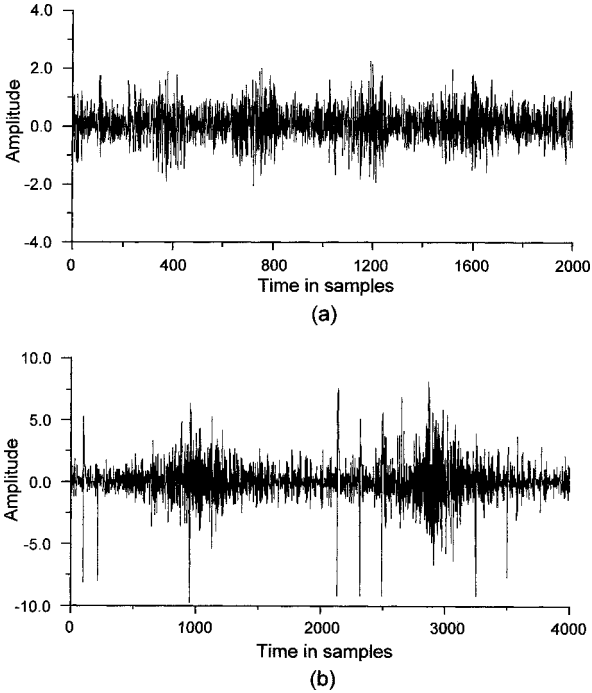

Figure 1. Typical examples of SEMG signals: (a) normal and (b) myopathies (sampling rate = 1000 samples/s).

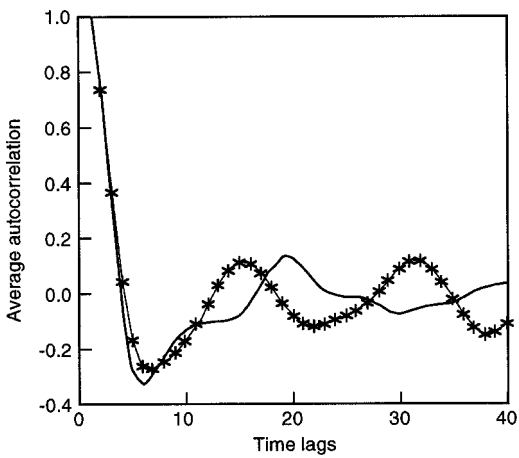

Figure 2. Typical average autocorrelation functions of the EMG signal recorded during 50% MVC for normal subject (—) and myopathic subject (***). The time interval between lags is 1 ms.

average autocorrelation functions of the two records. It can be seen that there is a significant correlation up to the second time lag. This time interval corresponds to a frequency value of about 500 Hz. Therefore, it is argued to choose a sampling frequency 1 kHz for diagnosis purposes.

3. AR MODELING OF THE SEMG

In the AR model each sample $emg(n)$ of the SEMG is described as a linear combination of previous samples plus an error term $e(n)$ that is independent of past samples, i.e.

$$emg(n) = -\sum_{k=1}^{p} a_k \cdot emg(n-k) + e(n) \tag{1}$$

where $emg(n)$ is the output model signal, a_k are the AR coefficients, $e(n)$ is the error sequence and p is the model order. The model represented by (1) can be used in a backward fashion (retrospective regression analysis); the signal at time n is considered as being the linear combination of p future values.

The system function is:

$$H(z) = \frac{1}{1 + \sum_{k=1}^{p} a_k \cdot z^{-k}} \tag{2}$$

$H(z)$ contains poles only. Thus, the model can work only for signals with a well-defined peaky spectrum and can be fitted to SEMG. The spectrum of the sequence $emg(n)$ can be estimated from the model if we consider $|E(\omega)| = 1$ (white noise sequence); therefore, the spectrum of the output signal is equal the spectrum of $H(z)$ and can be estimated by substituting $e^{-j\omega}$ into z as follows:

$$S(\omega) = |EMG(\omega)|^2 = \frac{1}{\left|1 + \sum_{k=1}^{p} a_k \cdot e^{-j\omega k}\right|^2} \tag{3}$$

The AR coefficients (a_k) are calculated using the covariance method [19] which minimizes the residual energy $\sum_n e^2(n)$.

3.1. Spectrum of the SEMG

The analysis was carried out on consecutive 500 ms segments of the EMG signal to ensure the stationarity of the segment where SEMG was found to be stationary on a segment length of less than 0.64 s [8]. Figure 3a demonstrates the spectrum of such segment calculated by a fast Fourier transform (FFT) routine. A consistent feature of EMG spectra is the existence of many spectral peaks in the region 10–200 Hz. The higher frequency regions, above 200 Hz, contain little minor amplitude information compared to the lower frequency region. Figure 3b demonstrates the spectrum of the AR model of the same signal calculated using 20 coefficients. It can be seen here that instead of obtaining six dominant peaks, only three peaks were obtained.

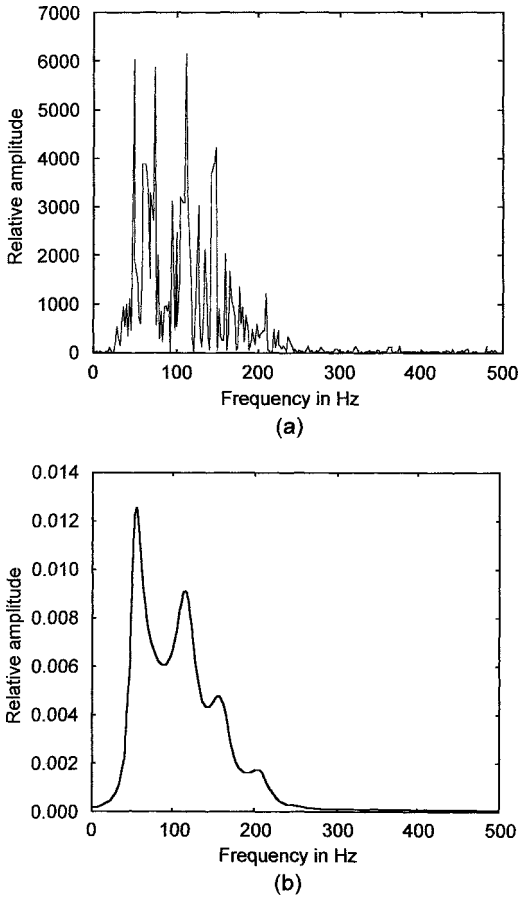

Figure 3. (a) Spectrum of Surface EMG segment calculated using FFT. (b) AR model spectrum for the same segment using 20 coefficients calculated using the covariance method.

3.2. Determination of the model order

The above model, instead of resolving nearby dominant frequencies, resolves frequencies in the high-frequency region that are minor to the dominant ones in the low region.

Figure 4 shows an attempt to resolve the problem of dominant frequencies by increasing the model order where the low frequency peak is still not pronounced. The model also tends to resolve the minor frequencies. It became apparent that most of the spectral components lie below 200 Hz as can be seen in Figs 3a and 4. This came in addition to poor spectral envelope matching which resulted from the inclusion of a higher-frequency band. It was decided, therefore, to disregard frequency components above 200 Hz and to reduce the bandwidth of the signal to one-half. The signals were filtered using a 230 Hz cut-off frequency and resampled at 500 Hz.

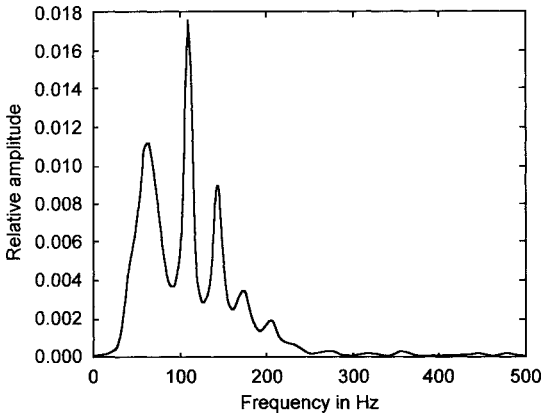

Figure 4. AR model spectrum of Fig. 3a with 30 coefficients.

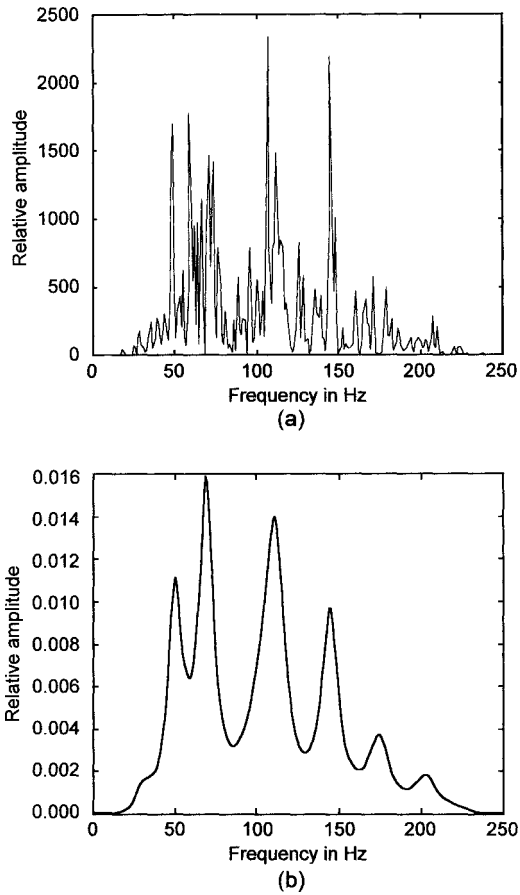

Figure 5. (a) The FFT spectrum of the EMG signal sampled at 500 Hz. (b) The AR model spectrum of the same EMG segment with 20 coefficients calculated using the covariance method.

Figure 5a demonstrates the FFT spectrum of the filtered signal (230 Hz). Figure 5b illustrates the spectrum of the all-pole 20 coefficients model with the EMG segment. It can be seen that most of the dominant frequencies are resolved and a much better spectral envelope fit is obtained. Therefore, a value of $p = 20$ was chosen to characterize surface EMG segments as a compromise between model size and accuracy of signal representation.

3.3. Determination of the number of segments

After characterizing each segment with 20 coefficients, it was observed from the calculation of the spectra of consecutive segments that the spectrum changes from segment to segment. Therefore, in order to determine how many segments would be enough to fully describe each subject, the average value of each coefficient was calculated and its convergence as a function of the number of segments was investigated. It has been shown that the changes in the values of the AR parameters become smaller after 10 segments. Therefore, it is argued to use 10 segments to characterize each subject; each segment is 500 ms long.

4. CLASSIFICATION OF THE SEMG

The classification approaches taken here are: the old Fisher linear discriminant [20] and ANN algorithms. Two paradigms for training the ANN are investigated, i.e. supervised and unsupervised. For supervised learning, the well-known back-propagation algorithm [21, 22], and for unsupervised learning, the SOM algorithms [23, 24], have been implemented. A comparison of the performance of the different classifiers is performed for normal and abnormal individuals. A training group of nine normals and nine myopathies, and a test group of five normals and five myopathies were used for ANN classifiers.

4.1. Fisher linear discriminant algorithm

The first step in the classification procedure is the construction of the Fisher linear discriminant vector (FLDV) W, where the two different classes $\Im_1$ and $\Im_2$ are introduced as in the following equation [24]:

$$W = C_{\mathrm{t}}^{-1}(\mu_1 - \mu_2) \tag{4}$$

where μ_1 and μ_2 are the means of the two classes $\Im_1$ and $\Im_2$, and C_{t} is the total *within-class covariance matrix* defined by

$$C_{\mathrm{t}} = \sum_{n \in \Im_1} (X_n - \mu_1) \cdot (X_n - \mu_1)^T + \sum_{n \in \Im_2} (X_n - \mu_2) \cdot (X_n - \mu_2)^T$$

After calculating the vector W, the projection of every subject that participates in the construction of the vector is first calculated and then the projection threshold

between the two different classes is determined. Using this threshold, the projection of unknown subjects is found and classified in accordance with the above threshold.

It has been found that the results are dependent on the number of participants in the construction of the FLDV. More participants mean better definition of the threshold between classes and thus better classification. Using nine normals and nine abnormals to construct the FLDV, a 60% percent successful classification was obtained for a test group of five normals and five abnormals.

4.2. Back-propagation neural network

The number of input nodes is 200 using the 20 AR coefficients for 10 SEMG segments and the number of outputs is one output node, where the output is corresponds to the two classes: normal and abnormal. The number of nodes in the hidden layers is changed (3–10 nodes) in order to determine the optimum number of nodes. A scaling method is used to scale the input patterns to give every pattern the same importance.

The results of classification using the back-propagation neural network trained with three different back-propagation algorithms are summarized in Tables 1–3. ANN architectures with three layers (input layer, hidden layer and output layer) were used [21, 22]. The ANN architectures are expressed as strings showing the number of inputs, the number of nodes in the hidden layers and one output node. The number of weights and the training time are tabulated for all models. During the training phase, an error measure of the closeness of weights to a solution can be calculated for each pattern (200 input features) that represents a subject in the training set. This measure is used for determining whether a certain subject has been learnt by the system and is defined by:

$$PSS = (y_l - d_l)^2 \tag{5}$$

where PSS is the Pattern sum squares, y_l is the calculated output and d_l is the desired output. The PSS measure is then summed over all patterns (18 subjects) to get the total sum of squares (TSS) measure:

$$TSS = \sum_{n=1}^{p} (y_l - d_l)^2 \quad n = 1, \cdots, p \tag{6}$$

where p is the number of training patterns (18 in this case; nine normals and nine abnormals).

The average error EE estimated for the output node:

$$EE = (TSS/p)^{0.5} \tag{7}$$

For comparing the results that were obtained by various classification algorithms, common performance metrics have been used [19]. For a given decision suggested by the output neuron, four possible alternatives exist: true positive (TP), false positive (FP), true negative (TN) and false negative (FN). A TP decision occurs

when the positive diagnosis of the algorithm coincides with a positive diagnosis according to the physician. A *FP* decision occurs when the algorithm made a positive diagnosis that does not coincide the physician. A *TN* decision occurs when the algorithm and the physician suggest the absence of a positive diagnosis. A *FN* decision occurs when the algorithm made a negative diagnosis that does not agree with the physician. From the above measures, correct classification percentage (*%CC*) has been calculated for the *N* cases in the evaluation set:

$$\%CC = 100 \times (TP + TN)/N \tag{8}$$

Important issues that characterize the overall performance of the back-propagation algorithms during the training procedure are:

(1) The output of all the back-propagation EMG models is limited between 1 and 0 range, so the selection of a sigmoidal activation function is preferred. The hidden layer nodes activation functions were also set to a sigmoidal function.

(2) At present, no method other than empirical has been proposed for choosing the architecture of feedforward neural networks so that for every training algorithm three architectures were created and compared.

(3) Training all the neural network models is accomplished using batch training.

(4) Networks of Table 1 are trained using a variable learning rate algorithm [25]. The first model architecture is insufficient to generalize the network where *Training %CC* $= 100$ but *Evaluation %CC* $= 70$. Models 2 and 3 are nearly suitable for generalization of the network. If we attempt to move towards a high architecture network, we will over fit the data and the network will be less generalized. The value of TSS will determine the generalization performance of the network, i.e. a high *EE* value will lead to a high *Training %CC* but less generalization where the network tends to memorize the training data; a small *EE* value will lead to best generalization but may be less *Training %CC*.

(5) All models of Table 2 are trained using variable a learning rate algorithm with an early stopping technique to determine the optimum value of *EE*. The available records are subdivided into two sets: training set and validation set. The problem of determining the suitable network architecture is removed using this technique. The number of epochs is reduced using an early stopping technique where the training will continue until validation test failure. In training the networks there is not sufficient records to form an evaluation data set, but with the first two sets the basic idea of early stopping technique is clarified.

(6) Table 3 is a backpropagation model trained with the *Conjugate Gradient Algorithm* [26]. Conjugate Gradient Training is faster than the old variable learning rate algorithm and is more suitable to large size networks than other fast algorithms. Therefore, it was found that it gives the highest performance for the present application.

Table 1.
The results of EMG classification using neural network back-propagation trained with variable learning rate

Model	Architecture	Weights	Epochs	*EE*	Time (s)	Training *%CC*	Evaluation *%CC*
1	200-3-1	603	323	10^{-5}	90	100	70
2	200-5-1	1005	328	10^{-5}	60	100	80
3	200-10-1	2010	285	10^{-5}	60	100	80

Table 2.
The results of EMG classification using neural network back-propagation trained with variable learning rate (early stopping technique)

Model	Architecture	Weights	Epochs	*EE*	Time (s)	Training *%CC*	Validation *%CC*
1	200-3-1	603	188	0.0047	30	90	90
2	200-5-1	1005	118	0.0532	30	90	90
3	200-10-1	2010	148	0.0067	45	100	90

Table 3.
Results of classification using neural network back-propagation EMG models trained with the conjugate gradient method and early stopping technique to improve generalization

Model	Architecture	Weights	Epochs	*EE*	Time (s)	Training *%CC*	Validation *%CC*
1	200-3-1	603	28	2.7×10^{-11}	25	100	80
2	200-5-1	1005	18	3×10^{-6}	20	100	90
3	200-10-1	2010	15	5.4×10^{-5}	20	100	90

4.3. SOM

The neural network models in this system were derived using Kohonen's SOM algorithm [27]. The algorithm creates a map of relationships among input patterns. The map is a reduced representation of the original data that preserves its topological relationships, i.e. the map has fewer dimensions but the clusters keep their relative positions. SOM creates the map from a random starting point without target results. SOM output nodes do not correspond to known classes but to unknown clusters that SOM finds in the data autonomously.

During the training process SOM finds the output node that has the least distance from the training pattern. It then changes the node's weights to increase its similarity to the training pattern. It also changes the weights of a block of adjacent nodes even though they have only random relationships to the training pattern. A wining neuron (node) thus influences its neighbors and different training patterns trigger different winners with different neighbors. The overall effect is to move the output nodes to

Table 4.
Results of using SOM classifiers

Model	No. of Inputs	No. of Classes	Output Grid	η	Epochs	Time (s)	Training %CC	Evaluation %CC
1	200	2	4×4	0.9	1000	75	944	60
2	200	2	6×6	0.9	1000	140	100	80
3	200	2	8×8	0.9	1000	270	100	80
4	200	2	10×10	0.9	1000	440	100	80

0	1	0	1	0	1
0	x	0	1	x	0
x	1	x	x	x	x
1	x	0	1	x	1
x	0	x	x	0	x
x	x	x	1	x	x

0	1	0	1	0	1
0	0	0	1	0	0
1	1	0	1	0	0
1	0	0	1	1	1
0	0	0	1	0	1
0	0	1	1	1	1

Figure 6. SOMs. (a) Maximum response map after training phase (100%). (b) Maximum response with all nodes assigned.

'positions' that map the distribution of the training patterns. After training, each node's weights model the features that characterize a cluster in the data, i.e. SOM finds natural clusters of feature similarities from unlabeled training data.

The results of the SOM models that were investigated with no preprocessing of the 200 input feature vector are summarized in Table 4. Models with output grid sizes (number of output nodes) of 4×4, 6×6, 8×8 and 10×10 were developed. The initial gain factor η was selected to be 0.9. It has been suggested [27] that the value of η should lie between 0 and 1, i.e. $0 < \eta < 1$. Training for SOM EMG models was carried out using 1000 epochs.

At each training cycle (epoch), the 18 training patterns were presented at random. It was observed that grid sizes below 6×6 were inadequate for producing models with well-separated classes. All models succeed in classifying all patterns during training phase, except for model 1.

The procedure that was followed for assigning normal and abnormal classes to the SOM is presented here.

For every 200 element feature vector:

$$x_n = [x_{1,n}, x_{2,n}, \cdots, x_{200,n}]^T, \quad n = 1, 2, \cdots, p \tag{9}$$

where p is the number of patterns in the training set ($p = 18$ patterns), there is an output node at the grid for which maximum response $R_{\max}$ is caused. This node is assigned the class number of the vector ($1 \rightarrow$ normal, $0 \rightarrow$ abnormal). Figure 6a shows the nodes where maximum response was caused by the patterns in the training set after the completion of the training phase.

0	1	0	1	0	1
0	0	0	1	0	0
1	1	0	1	0	0
1	0	0	1	1	1
0	0	0	1	0	1
0	0	1	1	1	1

(a)

		0			1
	1,0	0		0	
				1	
	0		1		
	1				

(b)

Figure 7. SOMs. (a) Simplified map showing the two classes boundaries. (b) Maximum response map for the evaluation set ($\%CC = 80$).

Nodes with '×' values have not been assigned to any class. For this model where the output grid is 6 × 6 (36 output nodes) with a training set of 18 patterns, at least 18 nodes will not be assigned to any pattern. This means that unknown patterns falling on '×' nodes will not be diagnosed.

During the next phase, the '×' nodes are assigned to one of the classes as follows. The data of each subject in the training set is applied at the input and the response at a certain '×' node is observed. The class of the subject that cause maximum response at the node is assigned to the node. This procedure is applied for all the '×' nodes until all of them are assigned to a class as shown in Fig. 6b. Figure 7a shows the two classes boundaries for all the nodes in the grid. Figure 7b shows the grid after the evaluation phase using the test group: five normal and five abnormal subjects which yield 80% correction classification ($\%CC$).

The SOM system compared to the back-propagation neural network system has the advantage of the results being presented pictorially, e.g. with this system one can relate a certain patient with another patient, find boundary cases and observe the mapping of a patient over serial examinations. Training efforts for SOM models was significantly reduced as compared to the back-propagation models.

4.4. PNN

The PNN is a Bayesian classifier put into a neural network architecture [28, 29]. It can be used as a function approximator like the back-propagation neural network.

The PNN should be used only for classification problems where there is a representative training set. It can be trained quickly but has slow recall and is memory intensive. It has solid underlying theory and can produce confidence intervals. This network is simply a Baysian classifier put into a neural network architecture. The PNN depends on the estimation of the probability density function for every class using the Gaussian weighting function:

$$g(x) = \frac{1}{n} \sum_{i=1}^{n} e^{-\frac{\|x - x_i\|^2}{2\sigma^2}} \tag{10}$$

Table 5.
Results of the PNN classifier

Spread (σ)	0.1	0.5	1	1.5	2
%CC	70	70	90	70	70

where n is the number of cases in a class, x_i is a specific case in a class, x is the input pattern to be classified and σ is the width parameter.

This formula simply estimates the probability density function (PDF) as an average of separate multivariate normal distributions. This function is used to calculate the PDF for each class.

The suggested PNN consists of three layers. When an input is presented, the first layer computes distances from the input vector to the training input vectors and produces a vector whose elements indicate how close the input is to a training input. The second layer sums these contributions for each class of inputs to produce as its net output a vector of probabilities. Finally, a compete transfer function on the output of the second layer picks the maximum of these probabilities, and produces a 1 for that class and a 0 for the other classes.

The PNN was used with no preprocessing. Eighteen training patterns and 10 test (evaluation) patterns with different σ (spread) were used and the results are shown in Table 5.

The effect of σ on the performance of the PNN is shown in Table 5 where other features may be looking for a training algorithm which train the spread coefficient to the optimum value like the weights of the networks.

5. DISCUSSION

5.1. Choice of AR model

In Section 3, an AR modeling method was described to characterize the surface EMG signal. The AR model, although it cannot be justified physiologically, can fit the SEMG because of its peaky spectrum nature. The covariance method was used for the calculation of the AR coefficients, and was found to be better in accuracy and computation speed compared to the autocorrelation method.

The choice of the model's order is discussed. In order to describe the spectrum of the SEMG (envelope), it has been found that a low-order model (2–6) is sufficient. However, in order to identify the motor unit firing rate, it has been found that the model order has to be about 30 (sampling rate = 1000 samples/s). This order can be reduced without loss of the resolution of the lower frequencies by decreasing the sampling rate or by using selective linear prediction. It is argued to use an AR model of order 20 to characterize surface EMG segments as a compromise between model size and accuracy of signal representation. The validity of the chosen order was confirmed by testing the whiteness of the residual signal, i.e. the difference between the original SEMG signal and the modeled version. A Kolmogorov–Smirnov one

sample test [30] was used and the results showed that there was no significant difference between the cumulative distributions of the two signals.

The SEMG was found to possess a changing spectral nature with a considerable variance. To overcome this spectral variability and to determine how many segments would be sufficient to fully describe each subject, the average value of each AR was calculated and its convergence as a function of the number of segments was investigated. The results showed that there was no change in the values of the coefficients for 10 segments or more. Therefore, it is argued to use 10 segments to characterize each subject, each segment is 500 ms long.

5.2. Classification

SEMG classification was performed using statistical and neural network classifiers. Three paradigms of ANN were investigated: the multilayer back-propagation algorithm, SOM algorithm and a PNN model. The performance of the three ANN classifiers was compared with that of the old FLD classifier. The ANN techniques performed better than the FLD and yielded a higher success rate. ANNs seem more appropriate for the classification of SEMG because of their ability to adapt and to create complex classification boundaries. The back-propagation neural networks presented in this study performed well even with a limited amount of data and achieved fast learning with a limited number of epochs. However, their performance depends on the learning algorithm. Networks trained with the variable learning rate method gives less percentage of correct classification than those trained using other learning algorithms. A 90% correct classification has been achieved using the conjugate gradient method or the early stopping technique.

The SOM investigated for the same real data required a much greater number of learning epochs in order to converge and gave 80% correct classification. However, SOM has the advantage of the results being presented pictorially. For example, one can relate a certain patient with another patient, find boundary cases and observe the mapping of the patient over serial examinations. The PNN performed well but its performance depends on the choice of the spread coefficient: a tuning procedure must be used in order to achieve the best results.

Further developments to the adopted ANN methodologies may be easily achieved by increasing the database used for training the neural networks and incorporating other muscle diseases. This is the aim of the next stage of work.

6. CONCLUSIONS

An attempt to characterize the SEMG for clinical classification was made. It has been demonstrated, that enough information remains in the recorded SEMG to allow its usage in clinical classification. An AR model was selected to characterize the signal since it reduces the dimensionality of spectral characterization.

ANN diagnosis models in conjunction with parametric analysis provide an integrated solution to the problem of automated EMG evaluation. This approach is

very desirable because it minimizes observer bias, facilitates comparisons of results across individual and different methodologies, and, more importantly, provides useful information for helping the physician in reaching a more accurate diagnosis.

The system presented here indicates that the SEMG, when properly processed, can replace needle EMG in some clinical applications and can be used to provide the physician with a diagnostic assist device. The amount of data collected until now is insufficient for making significant conclusions concerning the accuracy of classification. Yet it is suggested that the methods adopted have the potential of becoming an effective diagnostic device. This is only the first stage of a project aiming at building an expert system for SEMG. Adding new cases and new types of diseases seems to be the next and necessary steps.

REFERENCES

1. C. J. De Luca, Physiology and mathematics of myoelectric signals, *IEEE Trans.* **BME-26**, 313–325 (1979).
2. E. K. Richfield, B. A. Cohen and J. W. Albers, Review of quantitative and automated needle electromyographic analyses, *IEEE Trans.* **BME-28**, 506–514 (1981).
3. J.-L. Coatrieux, On-line electromygraphic signal processing system, *IEEE Trans.* **BME-31**, 199–207 (1984).
4. K. C. McGill, K. L. Cummins and L. J. Dorfman, Automatic decomposition of the clinical electromyogram, *IEEE Trans.* **BME-32**, 470–477 (1985).
5. E. A. Clancy and H. Hogan, Single site electromyography amplitude estimation, *IEEE Trans.* **BME-41**, 159–167 (1994).
6. T. D' Alessio, M. Knaflitz, G. Balestra and S. Paggi, On-line estimation of myoelectric signal spectral parameters and nonstationarities detection, *IEEE Trans.* **BME-40**, 981–984 (1993).
7. F. Tanzi and V. Taglietti, Spectral analysis of surface motor unit action potentials and surface interference electromyogram, *IEEE Trans.* **BME-28**, 318–324 (1981).
8. G. F. Inbar and A. E. Noujaim, On surface EMG spectral characterization and its application to diagnostic classification, *IEEE Trans.* **BME-31**, 597–604 (1984).
9. T. Kiryu, Y. Saitoh and K. Ishioka, Investigation on parametric analysis of dynamics EMG signals by a muscle-structured simulation model, *IEEE Trans.* **BME-39**, 280–288 (1992).
10. D. Graupe and W. K. Cline, Functional separation of SEMG signals via ARMA identification methods for prosthesis control purpose, *IEEE Trans.* **SMC-5**, 252–259 (1975).
11. M. H. Sherif, R. J. Gregor and J. Lyman, Effects of load on myoelectric signals: The ARIMA representation, *IEEE Trans.* **BME-28**, 411–416 (1981).
12. M. Capponi, T. D' Alessio and M. Laurenti, Sequential estimation of power spectra for nonstationary myoelectric signals, *Electromyogr. Clin. Neurophysiol.* **28**, 427–432 (1988).
13. T. Kiryu, C. J. De Luca and Y. Saitoh, AR modeling of myoelectric interference signals during a ramp contraction, *IEEE Trans.* **BME-41**, 1031–1038 (1994).
14. P. C. Doerschuk, D. E. Gustafon and A. S. Willsky, Upper extremity limb function discrimination using EMG signal analysis, *IEEE Trans.* **BME-30**, 18–29 (1983).
15. G. Hefftner, W. Zucchini and G. G. Jaros, The electromyogram (EMG) as a control signal for functional neuromuscular stimulation — Part II: practical demonstration of the EMG signature discrimination system, *IEEE Trans.* **BME-35**, 238–242 (1988).
16. J. L. Coatrieux, P. Toulouse, B. Rouvrais and R. Le Bars, Automatic classification of electromyographic signals, *EEG Clin. Neurophysiol.* **55**, 333–341 (1983).

17. M. H. Hassoun, C. Wang and A. R. Spitzer, Neural network extraction of repetitive vectors for electromyography. Part I and Part II, *IEEE Trans.* **BME-41**, 1039–1061 (1994).
18. C. S. Pattichis, C. N. Schizas and L. T. Middleton, Neural network models in EMG diagnosis, *IEEE Trans.* **BME-42**, 468–496 (1995).
19. S. M. Kay, *Modern Spectral Estimation.* Prentice-Hall, Englewood Cliffs, NJ (1988).
20. R. Duda and P. Hart, *Pattern Classification and Scene Analysis.* Wiley Interscience, New York (1975).
21. S. Haykin, *Neural Networks: A Comprehensive Foundation.* Prentice-Hall, Englewood Cliffs, NJ (1998).
22. R. Beale and T. Jacson, *Neural Computing: An Introduction.* Adam Hilger, Bristol (1990).
23. T. Kohonen, The self-organizing map, *Proc. IEEE* **78**, 1464–1480 (1990).
24. R. Schalkoff, *Pattern Recognition: Statistical, Structural and Neural Approaches.* John Wiley, New York (1992).
25. A. Cichocki and R. Unbehauen, *Neural Networks for Optimization and Signal Processing.* John Wiley, New York (1993).
26. W. H. Hines, *Matlab Supplement to Fuzzy and Neural Approaches in Engineering.* John Wiley, New York (1996).
27. J. Aleksander and H. Morton, *An Introduction to Neural Computing.* Chapman & Hall, London (1992).
28. L. Streit Roy and T. X. Luginbuhl, Maximum likelihood training of probabilistic neural networks, *IEEE Trans.* **NN-5** (9) (1994).
29. D. F. Specht, Probabilistic neural networks and the polynomial adaline as complementary techniques for classification, *IEEE Trans.* **NN-1**, 111–121 (1990).
30. S. Siegel, *Nonparametric Statistics for Behavioral Sciences*, McGraw-Hill, New York (1956).